Precise alignment method for MAORY

M. Patti* [a], M. Lombini [a], D. Magrin [d], M. Riva [b], E. Radaelli [b], D. Greggio [d], E. Diolaiti [a], F. Cortecchia [a], C. Arcidiacono [a], P. Ciliegi [a], P. Feautrier [c], R. Ragazzoni [d], S. Esposito [e].
[a]INAF – Osservatorio di Astrofisica e Scienza dello spazio, via Gobetti 93/3, 40129 Bologna (Italy); [b]INAF – Osservatorio Astronomico di Brera, Via E. Bianchi 46, 23807 Merate (Italy); [c]Institut de Planétologie et d'Astrophysique de Grenoble, 414, Rue de la Piscine, Domaine Universitaire, 38400 St-Martin d'Hères (France); [d]INAF – Osservatorio Astronomico di Padova, Vicolo Osservatorio 5, 35122 Padova (Italy); [e]INAF – Osservatorio Astrofisico di Arcetri, Largo E. Fermi 5, 50125 Firenze (Italy)

* mauro.patti@inaf.it ; phone +39 051 63573 315

ABSTRACT

MAORY (Multi-conjugate Adaptive Optics RelaY) and MICADO (MCAO Imaging CamerA for Deep Observations) will perform the science in the Multi-conjugate Adaptive Optics mode of the ELT (Extremely Large Telescope). One of their goals is the multi-object differential astrometry which requires low optical distortion and diffraction limited aberrations. To align MAORY, an automate method will be used during the integration of the instrument and could be part of the calibration strategy at the ELT site. This paper describes the method and the ray-tracing simulations carried out to validate the algorithm. Even in presence of different error sources, the method works in a large range of misalignments bringing the system close to the nominal performances.

--

Keywords: Alignment, Integration, Tolerance, Extremely Large Telescope, Optics, Ray-tracing

1. INTRODUCTION

MAORY [1] is the multi-conjugate adaptive optics (MCAO) module for the ELT [2] first light. It is a post-focal relay (PFR) optics [3] and will feed the high-resolution near-infrared imager and spectrograph MICADO [4] by offering two adaptive optics modes: MCAO and single-conjugate adaptive optics (SCAO).

At first light, MAORY will contain a single deformable mirror (DM) with provision for a second DM as an upgrade. The two or more DMs are conjugated to different altitudes to provide a wide Field of View (FoV) with high Strehl ratio and uniformity of the Point Spread Function (PSF).

In the MCAO mode, at least one DM within MAORY works together with the telescope adaptive mirror (M4). The MCAO mode is based on up to six Laser Guide Stars (LGSs) and three Natural Guide Stars (NGSs) for wavefront sensing. High Order (HO) wavefront sensing is performed by using LGSs while Low Order (LO) wavefront sensing is performed by using NGSs to measure the modes which cannot be accurately sensed by the LGSs. The six LGSs are produced by excitation of the atmospheric sodium with six laser beacons propagated from the edges of ELT pupil. The laser beacons work at wavelength of 589.2 nm and excite the sodium layer by optical pumping of the mesospheric sodium atoms.

The current baseline optical design of MAORY is based on six mirrors (including one or two DMs) and a dichroic beam-splitter. MAORY optics are optimized for the spectral band between 0.8 µm and 2.4 µm and the current optical design is shown in Figure 1. The dichroic beam-splitter is used to split the science light from the LGS light that is transmitted to the LGS Wavefront Sensors (WFSs) by means of a focusable objective [5].

MAORY is a big instrument with mirrors up to 1.2 m diameter placed on a bench of about 6m x 4m in plant. It is foreseen to operate at ambient temperature and exposed to environment effects such as earthquakes and seasonal temperature variation. These effects could cause a drift of the optical components from their nominal position beyond the tolerance range. The alignment algorithm, presented for the main path optics, is a powerful tool to restore the nominal optical performances and to reduce the amount of time allocated to some activities during the Assembly Integration and Verification (AIV) phase of MAORY.

The present document is focused on the alignment concept of the main path optics which relay the telescope focal plane to the exit ports for the science instruments (MICADO and 2nd instrument as yet undefined). The logic behind the method as well as the criteria in choosing compensators are described. A Monte Carlo approach has been used to simulate a range of optics mis-alignments considering also different error sources that affect the measurements.

2. MAORY MAIN PATH OPTICS

2.1 Opto-mechanical overview

The PFR optics of MAORY is a sub-system whose entrance focal plane is the ELT exit focal plane at the Nasmith-A straight through focus and produces three output ports:

1. the MICADO entrance focal plane;
2. the second port for a future instrument which is still undefined;
3. the image plane for the LGS WFS.

The baseline optical design of the main path optics, shown in Figure 1, consists of five mirrors with optical power (M6 to M10), a flat LGS Dichroic assumed to reflect the science light and flat 45º-tilted mirror (M11) which folds the light to the gravity-invariant port for MICADO. Mirrors numbering starts from 6 to take into the account the ELT five mirrors design. The second instrument port is achieved by inserting a flat folding mirror between M10 and M11.

Mirrors M8 and M9 are intended to be DMs for adaptive optics compensation of the optical wavefront. As such, they would be out of the scope of the present document. However, in a partial implementation of the instrument, at least the deformable mirror M9 would be replaced by a rigid mirror. For the scope of this document, they should be intended as rigid mirrors.

The mechanical support of the main path optics has been designed to hold the mirrors inside a barrel [6]. In order to sustain the loads, the mirror is positioned on several flexures. The flexures fix different degrees of freedom according to their position inside the mount. Each mount has two rotation axes: one azimuthal and one for the elevation (see Figure 2). Two kinds of gimbals permit the elevation and azimuthal rotation. It has the main advantage to be a stable, solid and repeatable mounting. A kinematic interface between the interface plate and the optical mount is foreseen with a repeatability of tens of microns. The position of the support points for each mount is optimized to minimize the optical surface deformation by itself weight and they are mounted radially in order to allow thermal breathing.

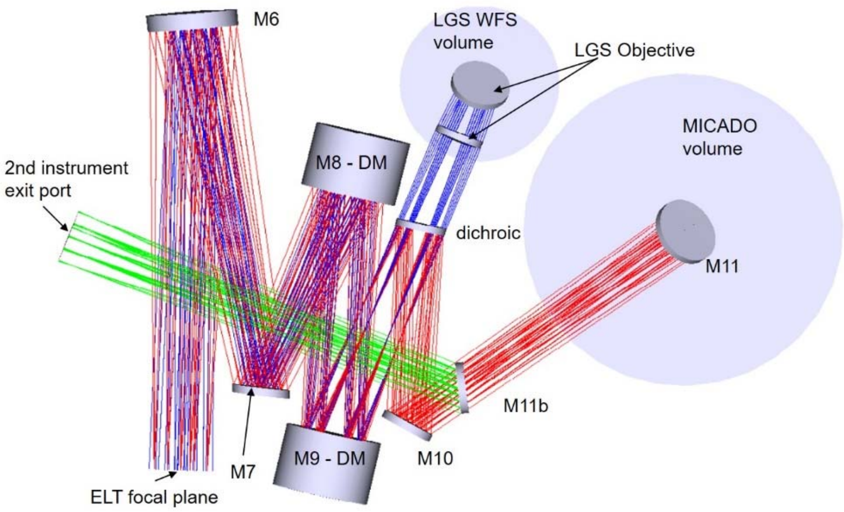

Figure 1. Post Focal Relay Optics layout. Red rays: optical beam from telescope focal plane to exit port for MICADO. Green rays: differential path to exit port for second instrument. Blue rays: LGS light to the objective.

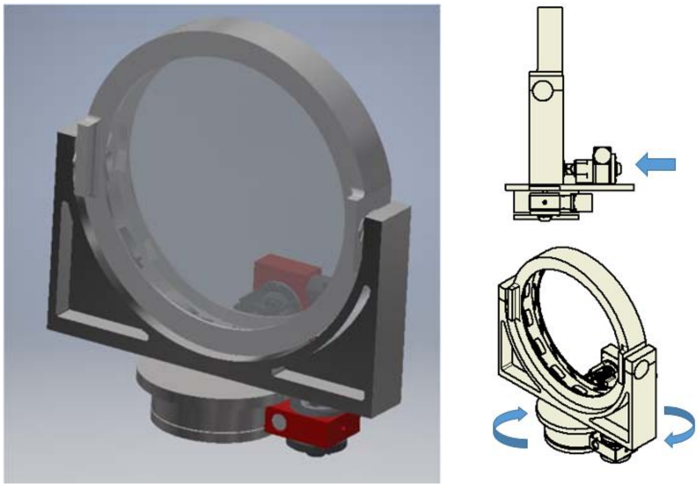

Figure 2. Panoramic of a general mount. Overall view of the two kind of gimbals which permit the elevation and azimuthal rotation.

3. MAIN PATH OPTICS ALIGNMENT

3.1 Alignment overview

The main path optical alignment concept is based on roughly positioning the optics within the precision of a laser tracker [7], then using active tip-tilt and axial adjustments to refine the alignment.
The laser tracker will be used as the global metrology system to survey and align every interface and to assembly and integrate every subsystem to the main structure.
It is important, as first step, to define a local and global coordinate system origin. The MAORY global coordinate system is the entrance focal plane. The FoV centre is the global origin. Each mirror has a local coordinate system whose origin is defined by the optical surface vertex. Spherically mounted retro-reflectors are the reference points used by the laser tracker. They will be installed on the optics and subsystems and their coordinates will be known with respect to the optics local coordinate system. These local coordinates will then be transferred into the MAORY global coordinate system.
Every interface in MAORY is designed to accept, at least, three retro-reflectors, creating a plane. These retro-reflectors define the local system of coordinate and they can be reached in a fast and repeatable way. The optical bench includes locations for the laser tracker to be mounted and features that accept the retro-reflectors at every interface.
Opto-mechanical components are assembled step by step starting with M11 and aligned to the optical reference by acting on the adjustment screws of the individual mounts. The laser tracker accuracy is valued to be around 50µm which is not enough to reach the required performances [8] and a more accurate alignment is necessary.
The main steps for the main path optics alignment are the following:

1. The optics are pre-aligned in their mounts prior to installation on the optical bench structure.
2. The laser tracker system reads the retro-sphere locations once the interface plate is installed on the optical bench. Then it is shimmed and settled into position according to the laser tracker measure.
3. Once the optics are properly located on the bench, they have to be aligned by using the compensators controlled by active components.

3.2 Compensators definition

The sensitivity analysis on opto-mechanical tolerance of MAORY [8] is a crucial step to plan the alignment concept that would be required in the AIV phase of the instrument. The analysis identified the worst offender Degrees Of Freedom (DOF) that are used as active compensators (Figure 3). Acting on these DOF, in principle, it is possible to compensate the performance degradation introduced by the other DOF misalignments. In reality, the active compensators are limited by mechanical accuracy and repeatability whose effect on performances has been allocated in the tolerances error budget [8].

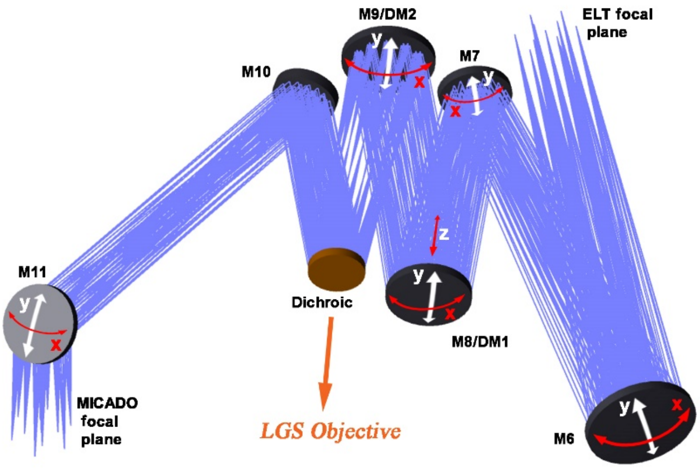

Figure 3. MAORY main path optics and its DOF compensators. Tilts on local x and y axes are necessary compensators to achieve diffraction limited optical quality during the alignment (plus one mirror axial distance Z). M11 tilts are additional compensators to align the exit pupil and center the optical axis on the de-rotator mechanical axis.

The DOF sensitivities are measured in terms of Zernike coefficients [9] across the field. By perturbing each of the individual DOF for each optical surface, the change of each Zernike coefficient is recorded in a matrix whose rows and columns are respectively the total number of Zernike values per field point and the total number of DOF. This sensitivity matrix includes all the necessary information to simulate the main path optics alignment using the best set of compensators. It is defined as:

$$S_{ij} = \partial Z_i / \partial x_j \tag{1}$$

Where the WFE is decomposed into *n* Zernike polynomials (Z_i; i=0, n) and the RSS of Z_i is the total WFE. $\partial Z_i/\partial x_j$ is measured from the nominal configuration as ($Z_{perturbed,i}$ - $Z_{nominal,i}$) while ∂x_j is the j^{th} DOF perturbation.
The worst offenders for optical quality, ordered from highest to lowest, are listed in Table 1 where the best set of mirrors, whose associated DOF are used as compensators, are highlighted in red.

Table 1. Most sensitive DOF to the main path RMS WFE. In red, the best set of mirrors used as compensators.

Degree of freedom	Optical element
X-Y Tilts	**M8** **M7** Dichroic **M6**
X-Y Decentres	M7
Axial position (Z)	**M8**

Since the dichroic transmits the light to the LGS Objective, an active compensation of this optical element, to align the main path optics, could introduce additional aberrations through LGS Objective. For this reason, the active compensation of the dichroic has been replaced by the one on M9. The sensitivity analysis demonstrates that a control on M8 axial position, in addition to the ELT re-focusing, is enough for focus compensation. The active control on M6, M7, M8 and M9 tilts is enough to compensate the WFE while the active control on M11 is foreseen to align both focal plane and exit pupil position as discussed later. Since there is no control on elements with optical power after the dichroic, the alignment of the main path optics is considered to be valid also for the LGS Objective at nominal design.
The worst offender for astrometry, in terms of misalignments, is the MAORY focal plane decentre with respect to the MICADO field de-rotator. In the real case, the FoV rotates at different speeds as the telescope tracks and a de-rotator is used to counter-rotate the field. During rotation, imaged sources don't follow a circle arc due to optical distortions. This introduces an error that propagates in the counter-rotation and translates in PSF elongation. In addition to intrinsic optical distortion, mirrors misalignments shift the optical axis in a way that it is no more aligned with the field de-rotator

mechanical axis. The mismatch generates star trails as shown in Figure 4 and can be compensated by tilting M11. That's the reason to add M11 tilts as additional compensators for geometric distortion. The tilts of M11, working in combinations with the other compensators, are also used to keep the exit pupil position at its nominal value.

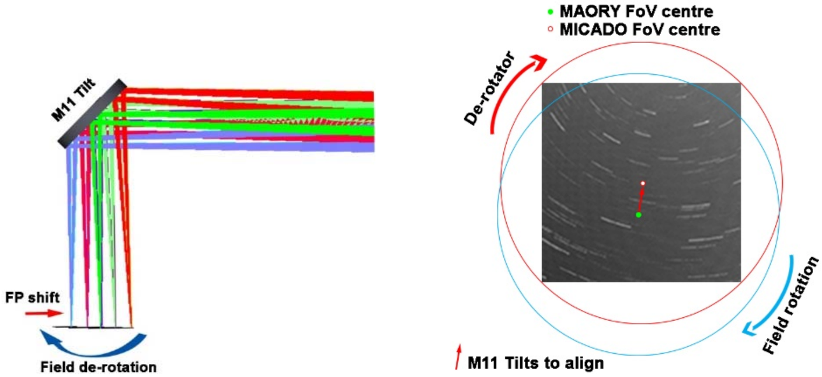

Figure 4. Geometric distortion due to field de-rotation errors. Focal plane shift w.r.t. rotational axis

3.3 Alignment tools

Two mechanical references are used to achieve the alignment:

1. Entrance port references to materialise ELT FoV and optical axis. This is the MAORY global coordinate system.
2. Exit port mechanical axis of a 'dummy' de-rotator. Any mechanical reference will be defined by a dummy field de-rotator which simulates the MICADO field de-rotator.

The MAORY FoV has to re-image the ELT focal plane with diffraction limited optical quality and low geometric distortion. A dedicated unit for calibration purposes is mandatory to simulate the ELT optical train in a 200 arcseconds FoV at Nasmyth focus of the telescope where MAORY is planned to be placed.
During the instrument AIV phase, some tests with multiple simulated stars in the laboratory is necessary to ensure the MCAO performances, calibrations and test the required control software. To exactly simulate a re-imaged star field by ELT, a set of artificial sources are placed at the entrance focal plane. The sources must be fixed with a proper chief ray angle to reproduce the telescope exit pupil position and should deliver 'diffraction limited' images. The surface connecting the fibres must be spherical with a curvature radius of 9,88 m. Figure 5 shows a conceptual layout for the sources in the image plane. ELT is not telecentric and the chief ray angle of a star changes along the pupil radius. Thus, at the focal plane, if the sources will be fixed on a circumference, they would have the same chief ray angle and the same sag (the component of the surface displacement from the vertex) reducing the complexity in terms of mechanical manufacturing.

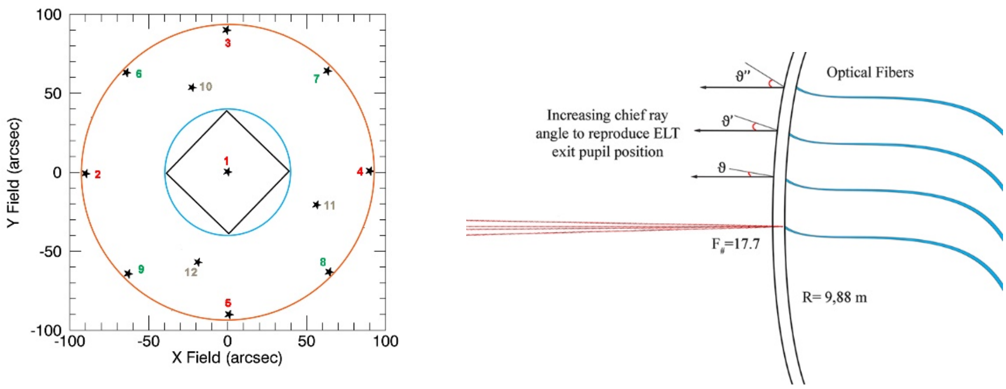

Figure 5. Conceptual layout for the sources (optical fibres) at the MAORY entrance focal plane to exactly reproduce the ELT focal plane. Left: x-y positions of the sources as seen by MAORY. Right: lateral view of the mask where the fibres should be plugged.

The NGS wavefront sensor (WFS) will be placed at the MAORY exit port. The MICADO dummy de-rotator and the NGS WFS can be considered as a single system aligned to the de-rotator axis.
At the beginning of MAORY alignment, the optical axis of the system must be defined. This axis has to be coincident with the rotation axis of the dummy de-rotator. The most confident approach is to materialize the de-rotator mechanical axis thanks to a laser beam placed at the global system coordinate origin.
The idea is to use tip-tilt adjustments by M11 mirror and centring adjustment by the laser with the assumption that the NGS WFS module is pre-assembled and aligned to the dummy de-rotator.
The main tools used to perform the alignment are:

- Laser beam.
- Commercial lenses.
- Beam splitter.
- Corner cube.
- Test camera.
- Reference flat mirror with cross-mark or another target on it.

The flat mirror is implemented as a reference inside the de-rotator bearing and equipped with tip-tilt regulations. A laser tracker is used to set the dummy de-rotator position to pre-align the reference mirror orthogonally to the rotator axis. A beam expander and a variable diaphragm allow, respectively, to adjust collimation and to select a small central portion of the laser beam to minimize aberrations.

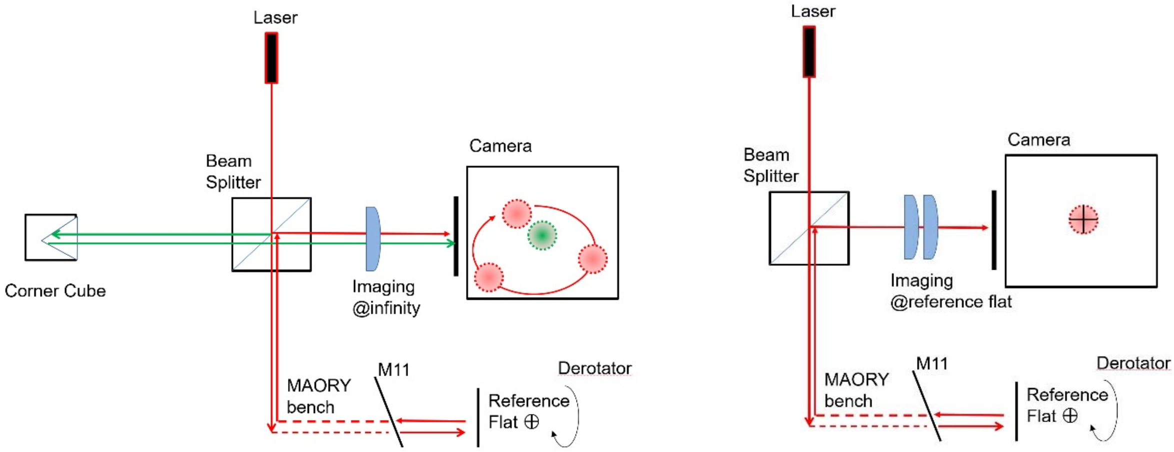

Figure 6. Left. First Camera configuration to remove spot rotation (adjust tip-tilt of reference flat) and to achieve the two spots overlapping (adjust the tip-tilt of M11). Right. Second camera configuration to center cross-mark (move laser beam on MAORY bench)

Referring to Figure 6, the beam splitter separates the light into the corner cube and the MAORY PFR direction. The beam coming from the reference mirror and the corner cube are re-combined and reflected into the lenses and test camera. The lenses role is to produce an imaging system for 2 configurations:

1. Tip-tilt corrections (focused to infinity).
2. Decentering correction (focused to plane of reference mirror with cross-mark).

The first phase of the alignment is leveling the de-rotator with respect to gravity and mount the reference flat mirror. With the camera in the first configuration, the corner cube reflects the incident laser beam in the same direction and produce a spot which is stationary during the field rotation. The reference mirror, if not properly co-planar with the de-rotator, produces a spot with elliptical trajectory whose axes are proportional to the mirror inclination respect to the rotation axis (see Figure 6, left). In this configuration, by adjusting the tip-tilt of the reference mirror, it is possible to detect a stationary spot when the mirror surface is perpendicular with the rotation axis. Then, by acting on the tip-tilt correction of M11, it is

possible to overlap the two spots. One reflected back by the reference mirror and the other (which is stationary) reflected by the corner cube. Now, the optical axis of MAORY is perpendicular with the de-rotator plane.
Switching to the second configuration of the camera, it is possible to adjust the laser beam to centre it on cross-mark (see Figure 6, right). At this point, the MAORY optical axis and the global system coordinate origin are defined. The fibre which simulates a re-imaged star by ELT at the centre of the FoV is positioned at the global system coordinate origin.

3.4 Optical alignment method

During the alignment phase, the Zernike coefficients are measured for different field points by means of a Shack-Hartmann wavefront sensor (SH-WFS). Let's consider the Zernike coefficients as a metric to evaluate the system performances (MF) and all the available compensators listed in a vector (x_c). The relation between the two can be written as:

$$\mathrm{MF} = f\,(x_c) \tag{2}$$

The goal is to find the best x_c that minimize MF. This relation could be non-linear and interdependences between DOF could occur.
The method implemented for MAORY is based on damped least squares algorithm of Zemax® ray-tracing software. Once a merit function for system performances is defined, the goal is to minimize the function:

$$\mathrm{MF}^2 = \frac{\sum W_i (V_i - T_i)^2}{\sum W_i} \tag{3}$$

Where V_i is the current value of each Zernike coefficient, T_i the target value, and W_i the weight. As previously described, the best set of compensators is defined by the sensitivity analysis and the compensators motions, that should be applied to align the system, are found by minimizing MF.
The measurements on Zernike coefficients are not enough to validate the alignment method. The main path optics is fully aligned when both focal plane and exit pupil positions are at their nominal values as well as the RMS WFE. To measure the exit focal plane position w.r.t. the de-rotator axis, one or more commercial cameras are placed at the main path optics focus to detect the centroids coordinates of the sources. The central field source defines the optical axis and it is also used to measure the pupil position. The flux within the Shack-Hartmann sub-apertures is a direct measure of the x, y coordinates of the pupil as shown in Figure 7.

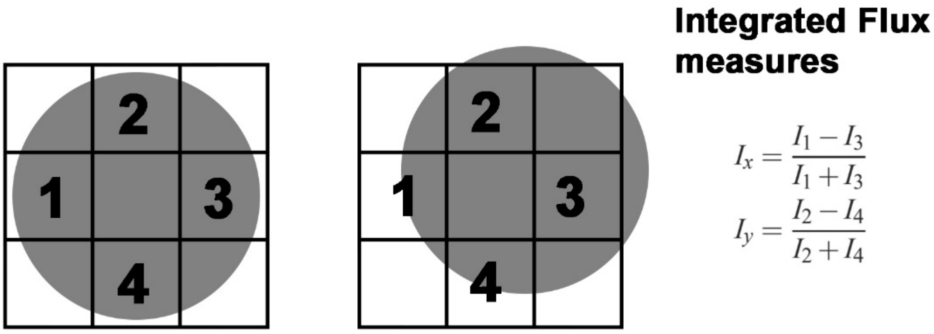

Figure 7. Schematic representation of the pupil shift measurement using the Shack-Hartmann lenslet array.

Considering four areas at the extremities of the x, y axes of the lenslet array (see Figure 7), the integrated flux of each area is defined as I_i (i from 1 to 4). If d is the length of the sub-aperture side which defines the area, the x,y coordinates shift of the pupil are:

$$x = \frac{I_1 - I_3}{I_1 + I_3}\, d \quad ; \quad y = \frac{I_2 - I_4}{I_2 + I_4}\, d \tag{4}$$

The V_i and T_i values of equation 3, in addition to Zernike coefficients, are also centroids coordinates of the sources and the exit pupil coordinates of the central field. In principle, the centroid coordinates of the central field are enough to align the exit focal plane, but we plan to use more field points to better constrain the merit function and reduce the errors.

The developed alignment algorithm is based on Zemax Programming Language (ZPL) macros and operates as follow:

1. Zernike coefficients, sources centroids and pupil position of the nominal design are the references → V_i
2. Assemble the main path optics with the laser tracker accuracy.
3. Measure the Zernike coefficients from the SH-WFS located at different focal points → T_i
4. Measure the centroids coordinates from cameras located at different focal points → T_i
5. Measure the exit pupil coordinates of the central field → T_i
6. Allocate all the measured values to target column in the merit function editor of the nominal design.
7. Optimize the system using the Zemax damped least squared algorithm and add M11 tilts as variables if necessary.
8. Read the perturbed compensator DOF. These are the motions that should be applied in a reverse way to achieve the main path optics alignment.

3.5 Main Path Optics nominal design performances

The RMS WFE at the exit focal plane of the Main Path Optics is shown in Figure 8. MICADO will use a 75 arcsec diameter FoV where diffraction limited performances without atmospheric turbulence must be guaranteed. The off-axis mirrors are decentred and tilted in one axis only, hence the WFE map is symmetric along the other axis.

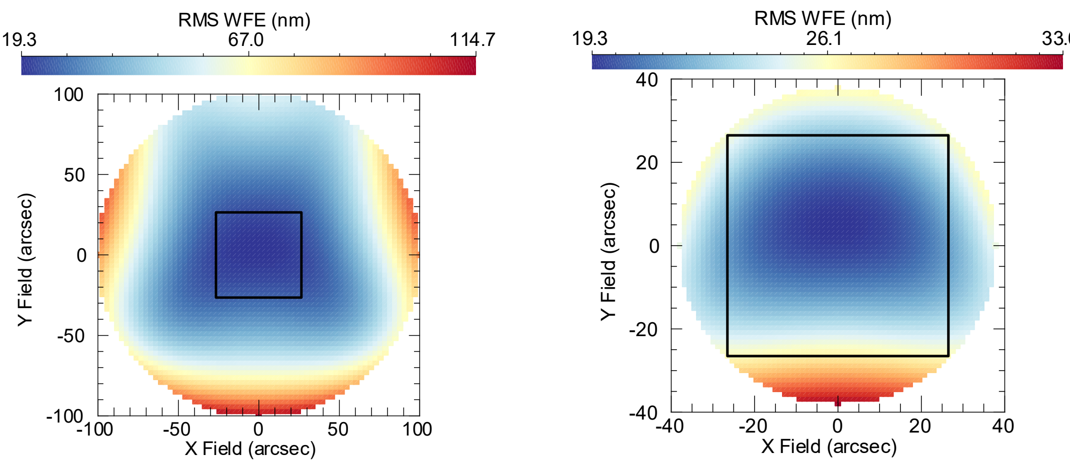

Figure 8. RMS WFE without degradation from manufacturing and alignment errors; nominal telescope design included. Left: RMS WFE maps of the entire MAORY FoV. Right: RMS WFE maps of MAORY within the MICADO FoV. The black square is the 53”x53” MICADO detector.

The distortion analysis considers the maximum integration time for narrow band astrometric observations at 80° of telescope elevation, i.e. 10° from zenith. For wavelength λ = 1µm, the amount of distortion shall be < 2.4 mas at the MAORY exit focal plane on the MICADO FoV (F/17.74 focal ratio).
The positions of a set of N test stars placed over a regular grid has been used to evaluate the geometric distortion. Let us define X_1, Y_1 the initial coordinates of star centroids. X_2, Y_2 the coordinates of the star centroids after the maximum astrometric exposure time (i.e. 2.6° FoV rotation and counter-rotation angle). The PSF centroids move, because of geometric distortions, by $\Delta X = (X_2 - X_1)$ and $\Delta Y = (Y_2 - Y_1)$. The vector sum of ΔX and ΔY is the geometric distortion shown in Figure 9. Besides intra-epoch observations, MAORY has a requirement on the inter-epoch observations where a n^{th} order polynomial fit is used to model and correct optical distortions [8]. Since the misalignments are a LO contribution to optical distortions, a 3^{rd} order polynomial correction is able to retrieve the nominal performances. Thus, to validate the alignment, the method presented in this document will consider the distortion requirement on intra-epoch observation.
In an ideal world, the alignment procedure should be able to achieve the nominal performance. In the real world, the accuracy of active compensators will set a limit to the achievable performances by the alignment procedure. The expected performances are those given by the alignment tolerances described in Patti et al. [8].

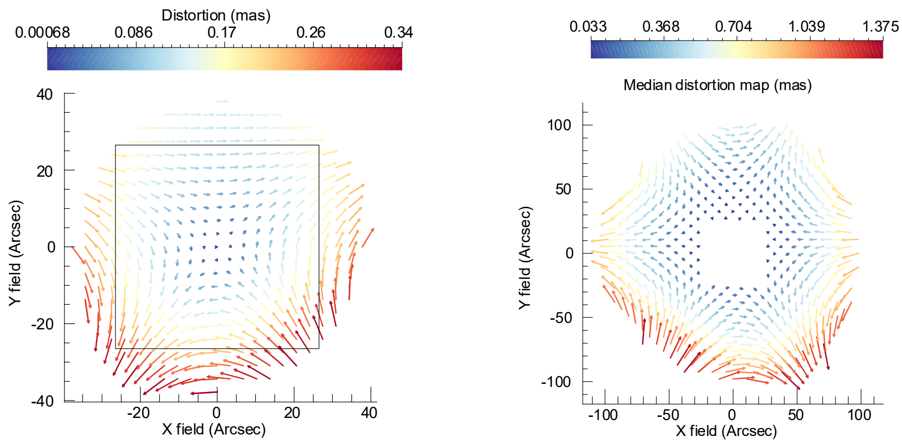

Figure 9. Distortion map at the exit port within the maximum integration time for narrow band astrometric observations (without degradation from manufacturing and alignment errors; nominal telescope design included). Left: Distortion map in the circle containing the MICADO FoV (black square). Right: Distortion map in the NGS patrol FoV

4. ALIGNMENT SIMULATIONS

To test the Zemax-based algorithm, 500 Monte Carlo trials were run simulating random misalignments consistent with the laser tracker accuracy. The Monte Carlo trials follow a parabolic distribution for considered DOF misalignments. The extremes of misalignments range assigned to the DOF are as follow:

- XYZ positions = ± 0.1 mm
- XYZ tilts = ± 0.1 mrad

For each Monte Carlo trial, the DOF which have a specified nominal value are randomly perturbed using the defined range of misalignments and the statistical model of the parabolic distribution over the specified range. The parabolic distribution yields selected values that are more likely to be at the extreme ends of the tolerance range, rather than near the middle as for a gaussian distribution. Figure 13 is an example of parabolic distribution.

Figure 10 shows the starting point in terms of RMS WFE of the main path optics through the Monte Carlo trials. Given the same set of 500 Monte Carlo trials, the alignment simulation was run several time varying different parameters. This approach was adopted to analyse all possible error sources that could affect the measurements and the accuracy of the algorithm. The variable parameters among different alignment simulations are the following:

- Field sampling: related to the number and geometry of the sources.
- Errors on sources position w.r.t. the nominal stars position on sky.
- Errors on pupil position measurements.
- Errors on WFS measurements: related to uncertainties in the measured Zernike coefficients.
- Mirror surfaces irregularities: related to uncertainties in the measured WFE data of mirror surface.

To take care of these errors, during the reverse optimization, the nominal sources positions are considered as variables in addition to the DOF used as compensators.

To give an idea of the algorithm effectiveness, Figure 11 shows the results of the alignment procedure in terms of RMS WFE through the aligned Monte Carlo trials (see Figure 8 for comparison). In this case, no errors were considered and nine sources (eight at the edge of the FoV and one at the centre) were used to detect the observables.

The results from Monte Carlo trials reveal that 95% of aligned systems are within 1 nm of residual RMS WFE (mean across the entire FoV) and within the limits for optical distortions. The worst Monte Carlo trial, in terms of maximum distortion value, reaches about 0.6 mas at the edge of MICADO FoV after the alignment.

The criteria followed to evaluate the alignment accuracy are as follows:

1. Residual mean RMS WFE. It is the difference between the nominal WFE and the measured WFE (mean across the entire FoV) after the alignment procedure.
2. Residual intra-epoch distortion. It is the difference in terms of the maximum PSF blur due to distortion at the edge of MICADO FoV between the nominal value and the measured value after the alignment procedure.
3. Residual exit pupil position. It is the difference, in percent of the exit pupil diameter, between the nominal position and the measured position after the alignment procedure.

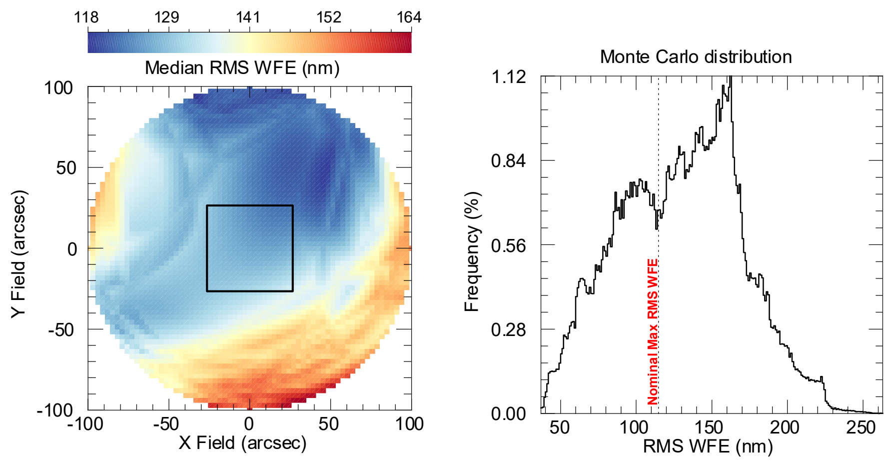

Figure 10. Black square is the MICADO 53"x53" FoV. Right: 2D RMS WFE map of median values given by the Monte Carlo trials that simulate system misalignments. Left: distribution of values given by the Monte Carlo trials. The maximum RMS WFE of the nominal design is shown as threshold for reference.

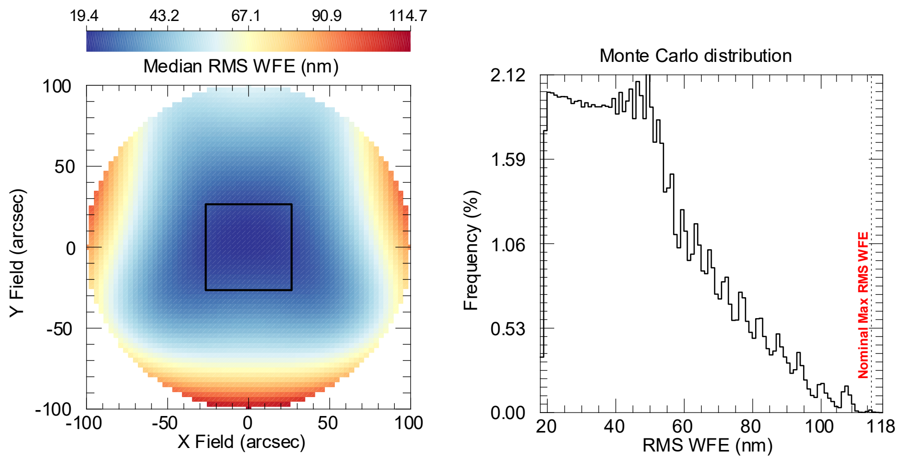

Figure 11. Same of Figure 10 but after the error-free alignment simulation.

4.1 Field sampling

Field sampling should be considered to address the best ratio of alignment performance and number of sources. Since the artificial source must reproduce the ELT focal plane with the right exit pupil position, different geometries of sources were investigated to find the most reliable in terms of mechanical manufacturing. ELT is not telecentric and the chief ray angle of a star changes along the pupil radius. As discussed in section 3.3, at the focal plane, if the sources will be fixed on a circumference, they would have the same chief ray angle reducing the complexity in terms of mechanical manufacturing. The considered sources number and geometry are shown in Figure 5 (left). The simulation was run considering three different set of 5, 9 and 12 sources. The results are summarized in in terms of mean residual RMS WFE over the entire FoV. Boxplots are the distributions of values across the 500 Monte Carlo trials. The number of sources is not a sensitive parameter to reach the intra-epoch astrometry requirement. If no errors are considered, a single central source is enough to align the exit focal plane to the de-rotator axis with residuals < 0.6 mas.

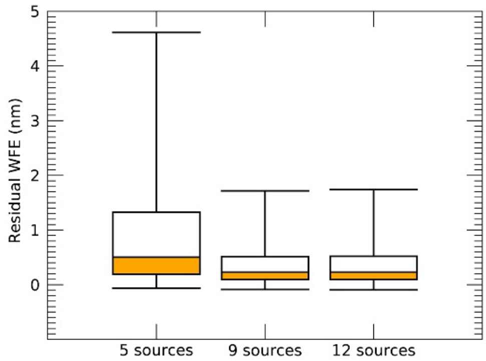

Figure 12. Residual RMS WFE. It is the difference between the nominal WFE and the measured WFE (mean across the entire FoV) after the alignment procedure. Box plots show minimum and maximum values and quartiles of Monte Carlo trials distribution

4.2 Measurement errors

Once the optimal number of sources has been defined, the alignment simulation was run considering measurement errors of values which are used as target for the merit function. The observables, extrapolated from the Monte Carlo trials, have been perturbed by systematic errors in the range of:

1. ± 5.4 µm as error on centroids coordinates. This correspond to about one pixel of commercial CCD camera (KODAD KAF-8300) and it is coherent with the centroid accuracy due to detector noise.
2. ± 0.1% of the pupil diameter as error on pupil position. This correspond to the tolerance on pupil position.
3. ± 10 nm as error on each Zernike coefficient. This correspond to a conservative accuracy of the WFS.

A parabolic distribution for each range of errors has been considered as show in Figure 13 (e.g. the error on Zernike coefficients). Source position errors should be considered as part of tolerance in mechanical manufacturing of the mask that simulates the ELT focal plane. To take care of these errors, during the reverse optimization, the nominal sources positions are considered as variables in addition to the DOF compensators.

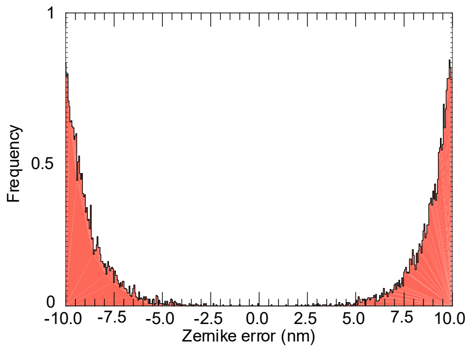

Figure 13. Parabolic distribution of Zernike coefficients error. Same distribution has been used in the range of other errors.

The results of simulation are shown in Figure 14. Despite errors on WFS measurements, the main path optics achieves the alignment with low residuals on the mean RMS WFE (< 4 nm). The mean of the residuals distribution for the exit pupil position is equal to the introduced error, as expected. The mean of the residuals distribution for the intra-epoch distortion is consistent with the differential rotation of a source at the edge of the MICADO FoV when the focal plane is shifted by ± 5.4 µm w.r.t. the de-rotator axis.

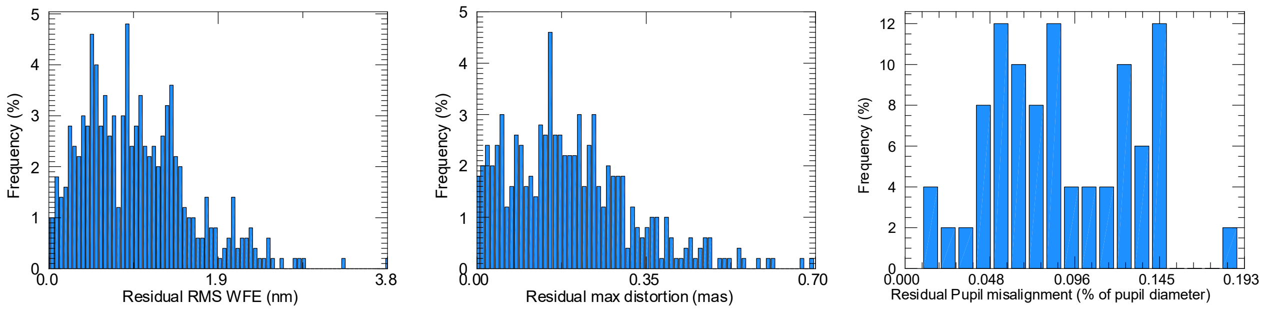

Figure 14. Distribution of residual values (difference between nominal and aligned system). From left to right: mean RMS WFE, max intra-epoch distortion at the edge of MICADO FoV and exit pupil position in percent of its diameter.

4.3 Mirrors irregularities

MAORY mirrors are planned to be delivered by the companies with a full characterization of mirror surfaces. In principle, we can use the measured values of surface irregularities and add this information to the nominal design. In case we miss this information, or they are not accurate, the impact of surface irregularities on the robustness of the alignment procedure is shown in Figure 15.

The irregularities were modelled by means of 54 standard Zernike coefficients [9] whose square root of the sum of the squares yields the specified RMS value. Low order irregularities (Zernike coefficient < 12) are partially absorbed during the alignment, while high order irregularities are critical for the algorithm accuracy. A good characterization of mirror surfaces is required for a successful MAORY alignment.

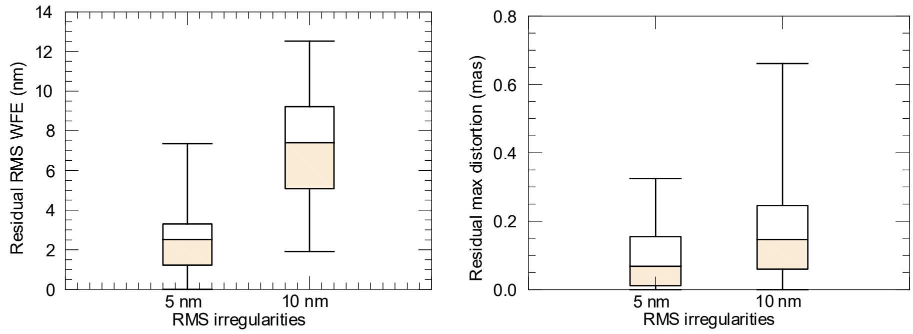

Figure 15. Difference between the nominal WFE and the measured WFE (mean across the entire FoV) after the alignment procedure when uncertainties on mirrors surfaces shapes are considered. 5nm and 10nm are the exact RMS error of each surface. Box plots show minimum and maximum values and quartiles of Monte Carlo trials distribution.

5. CONCLUSIONS

The alignment method, presented for the main path optics, is independent from the optical design and it is a powerful tool to reduce the amount of time allocated to some activities during the AIV phase. Since the method is fully automatic, it could be used to actively control MAORY optics at ELT site during maintenance or calibration operations. The ray-tracing simulations verified that such method is able to recover the nominal optical performances with negligible residuals on WFE and optical distortions. Different error sources that could increase the algorithm uncertainty have been considered. The worst offenders to the alignment accuracy are optical surface irregularities implying a good characterization of manufactured mirrors is required. The raytracing simulations that have been run to validate the alignment method, had a crucial role to define the minimum requirements on the geometry and number of sources for the calibration unit.

6. RIFERENCES

[1] E. Diolaiti e M. A. O. R. Y. Team, «MAORY for ELT: preliminary design overview,» in *Adaptive Optics Systems VI*, 2018.

[2] R. Gilmozzi e J. Spyromilio, «The 42m european elt: status,» in *SPIE Astronomical Telescopes+Instrumentation*, 2008.

[3] M. Lombini, D. Magrin, M. Patti, D. Greggio, F. Cortecchia, E. Diolaiti, V. De Caprio, A. De Rosa, E. Radaelli, M. Riva, P. Ciliegi, S. Esposito, P. Feautrier e R. Ragazzoni, «Optical design of the post focal relay of MAORY,» in *SPIE Optical Design and Engineering VII*, 2018.

[4] R. Davies e M. I. C. A. D. O. Team, «MICADO: the E-ELT adaptive optics imaging camera,» *arXiv preprint arXiv:1005.5009,* 2010.

[5] M. Lombini, «Laser Guide Star Objective of MAORY,» in *Proceedings of the Adaptive Optics for Extremely Large Telescopes 5*, 2017.

[6] M. Riva, E. Redaelli, M. Aliverti e t. al., «Optomechanical design of Maory post focal relay optics,» in *SPIE Ground-based and Airborne Instrumentation for Astronomy VII*, 2018.

[7] J. H. Burge, P. Su, C. Zhao e T. Zobrist, «Use of a commercial laser tracker for optical alignment,» *Proc. of SPIE,* vol. 6676, p. 66760E.

[8] M. Patti, M. Lombini, D. Magrin, D. Greggio, E. Diolaiti, F. Cortecchia, C. Arcidiacono, P. Ciliegi, P. Feautrier, R. Ragazzoni e S. Esposito, «MAORY optical design analysis and tolerances,» in *SPIE Optical Design and Engineering VII*, 2018.

[9] R. J. Noll, «Zernike polynomials and atmospheric turbulence,» *JOsA,* vol. 66, pp. 207-211, 1976.